Electrically tunable laser based on oblique heliconical cholesteric liquid crystal

Jie Xiang[a,b], Andrii Varanytsia[a,b], Fred Minkowski[a,b], Daniel A. Paterson[c], John M. D. Storey[c], Corrie T. Imrie[c], Oleg D. Lavrentovich[a,b,1], and Peter Palffy-Muhoray[a,b,1]

[a]Liquid Crystal Institute, Kent State University, Kent, OH 44242; [b]Chemical Physics Interdisciplinary Program, Kent State University, Kent, OH 44242; and [c]Department of Chemistry, School of Natural and Computing Sciences, University of Aberdeen, Aberdeen AB24 3UE, Scotland, United Kingdom

Edited by Timothy M. Swager, Massachusetts Institute of Technology, Cambridge, MA, and approved October 5, 2016 (received for review July 24, 2016)

A cholesteric liquid crystal (CLC) formed by chiral molecules represents a self-assembled one-dimensionally periodic helical structure with pitch p in the submicrometer and micrometer range. Because of the spatial periodicity of the dielectric permittivity, a CLC doped with a fluorescent dye and pumped optically is capable of mirrorless lasing. An attractive feature of a CLC laser is that the pitch p and thus the wavelength of lasing $\bar{\lambda}$ can be tuned, for example, by chemical composition. However, the most desired mode to tune the laser, by an electric field, has so far been elusive. Here we present the realization of an electrically tunable laser with $\bar{\lambda}$ spanning an extraordinarily broad range (>100 nm) of the visible spectrum. The effect is achieved by using an electric-field-induced oblique helicoidal (OH) state in which the molecules form an acute angle with the helicoidal axis rather than align perpendicularly to it as in a field-free CLC. The principal advantage of the electrically controlled CLC_{OH} laser is that the electric field is applied parallel to the helical axis and thus changes the pitch but preserves the single-harmonic structure. The preserved single-harmonic structure ensures efficiency of lasing in the entire tunable range of emission. The broad tuning range of CLC_{OH} lasers, coupled with their microscopic size and narrow line widths, may enable new applications in areas such as diagnostics, sensing, microscopy, displays, and holography.

cholesteric liquid crystals | lasing | electric tunability | heliconical structure

Chiral interactions in cholesteric liquid crystals (CLCs) result in supramolecular helical structures (1). The nematic director $\hat{\mathbf{n}}$ defining molecular orientation is perpendicular to the helix axis and rotates continuously along the axis, generating a regular right-angle helix with pitch p. Because the dielectric tensor is periodic in space, the CLC is a 1D photonic bandgap structure, selectively reflecting circularly polarized light of the same handedness as the helix. The reflection band edges are at wavelengths $\lambda_o = pn_o$ and $\lambda_e = pn_e$, where n_o and n_e are, respectively, the ordinary and extraordinary refractive indices of the local uniaxial structure (1).

In optically pumped thin layers of CLCs doped with fluorescent dyes, selective Bragg reflection of light gives rise to mirrorless lasing at the reflection band edges. Early demonstrations of lasing from CLCs (2–6) stimulated considerable interest in these easily produced micrometer-sized laser light sources due to their potential in spectroscopic, communications, sensing, and display applications. One major appeal of CLC lasers is the tunability of the emission wavelength by controlling the pitch. This can be achieved by changing the temperature (6–8), composition or cell thickness (9–11), mechanical strain in cross-linked CLC elastomers (12–14), and using reversible photochemical reactions (15, 16). The most sought-after control is via an applied electric field, which, although possible in principle (17–23), has not yet achieved its full potential. The principal difficulty is created by the very geometry of CLC in which the molecules are oriented perpendicularly to the helical axis, as explained below.

CLC molecules tend to align parallel to an electric field $\mathbf{E}$ if the local dielectric anisotropy is positive, $\varepsilon_a = \varepsilon_{||} - \varepsilon_{\perp} > 0$ (the subscripts refer to the direction with respect to $\hat{\mathbf{n}}$). When $\mathbf{E}$ is nearly parallel to the helical axis $\hat{\mathbf{h}}$, it tends to rotate the axis. Once $\hat{\mathbf{h}}$ is perpendicular to $\mathbf{E}$, the field expands the regions where $\hat{\mathbf{n}}$ is parallel to $\mathbf{E}$, thus introducing higher spatial harmonics into the structure. Such a distorted structure creates additional reflection bands at higher frequencies (24) and dramatically reduces the laser emission intensity (21, 25). Similar distortions occur not only in CLCs but also in chiral smectic C lasers when the applied field is perpendicular to the $\hat{\mathbf{h}}$ axis (18). The electric field tunability of CLC lasers is therefore severely limited (17). An ideal electrically tunable CLC laser would be the one in which the electric field modifies only the pitch, but preserves the otherwise undistorted helical structure.

In this work, we describe such a laser, based on the oblique helicoidal (CLC_{OH}) state of certain CLCs. The director in a CLC_{OH} structure rotates about the helical axis as in conventional CLCs, but instead of being perpendicular to $\hat{\mathbf{h}}$, it makes an acute angle θ with the axis, as shown in Fig. 1 *A* and *B*. When the electric field is applied parallel to the helicoidal axis, $\mathbf{E} \parallel \hat{\mathbf{h}}$, and increases, the molecules tend to align along the field, thus reducing the angle θ and, as shown both theoretically (26, 27) and experimentally (28, 29), reducing the pitch, $p \propto 1/E$ (Fig. 1 *A* and *B*). Importantly, the field-induced changes of θ and p do not change the orientation of $\hat{\mathbf{h}}$, which remains parallel to the applied field and so the single-harmonic periodic nature of CLC_{OH} does not change (28, 29). Here we demonstrate lasing in CLC_{OH} structures and an extraordinary broad range of electrical tuning of the emission wavelength $\bar{\lambda}$, on the order of 100 nm.

The CLC_{OH} structure is formed in CLC materials with a very small bend elastic constant K_3 under the influence of an electric

Significance

Liquid-crystal lasers based on micrometer-scale self-organization of organic molecules into the so-called cholesteric liquid crystal are simple to manufacture; they are small in size and low in cost and power consumption. Their potential applications range from sensing and imaging to informational displays and miniature "lab-on-a-chip" devices. We report a cholesteric structure used as the laser's resonator cavity that enables a continuous real-time tuning of the emitted wavelength in a very broad range by applying an electric field. The structure is heliconical, with the molecules rotating around a helical axis and being tilted toward this axis. The electric field controls the tilt and the pitch, thus changing the wavelength by at least 100 nm.

Author contributions: O.D.L. and P.P.-M. designed research; J.X., A.V., and F.M. performed research; D.A.P., J.M.D.S., and C.T.I. contributed new reagents/analytic tools; O.D.L. and P.P.-M. analyzed data; D.A.P., J.M.D.S., and C.T.I. synthesized the materials; and O.D.L. and P.P.-M. wrote the paper.

The authors declare no conflict of interest.

This article is a PNAS Direct Submission.

Freely available online through the PNAS open access option.

[1]To whom correspondence may be addressed. Email: olavrent@kent.edu or mpalffy@kent.edu.

This article contains supporting information online at www.pnas.org/lookup/suppl/doi:10.1073/pnas.1612212113/-/DCSupplemental.

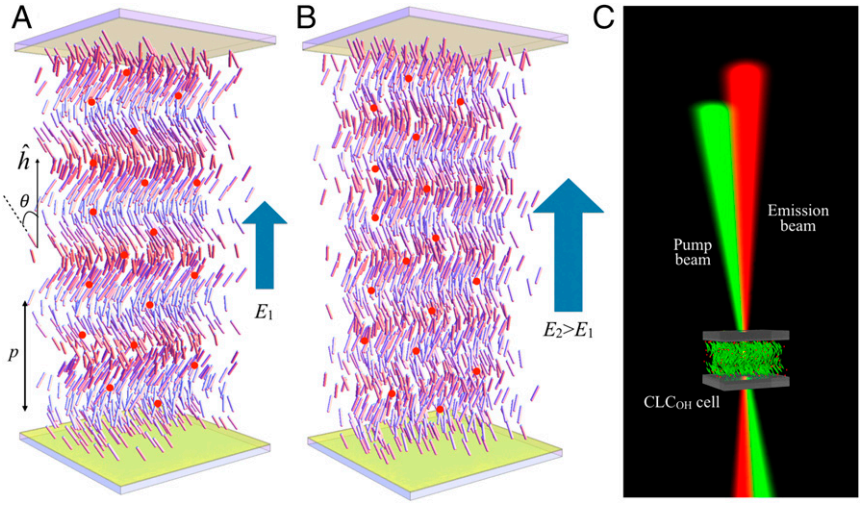

Fig. 1. Schematic of electrically tunable lasing in dye-doped cholesteric heliconical structure. (*A*) Electrically tunable CLC_{OH} structure with lasing emission. (*B*) Increase of the field leads to shortening of the pitch and decrease of the cone angle. (*C*) Schematic of lasing cell with pump and laser emission beams. Red spheres and green ellipsoids represent dye molecules and LC molecules, respectively.

field, as predicted by Meyer (27) and de Gennes (26), and as observed in Raman–Nath diffraction (28) and Bragg reflection (29) experiments. ChC_{OH} materials are typically formed by mixing dimeric molecules (representing two rigid rod-like units connected by a flexible chain) with chiral additives (28, 29). We used a mixture comprising two dimeric LCs, 1′,7′-bis(4-cyanobiphenyl-4′-yl)heptane (CB7CB) and 1-(4-cyanobiphenyl-4'-yl)-6-(4-cyanobiphenyl-4'-yloxy)hexane (CB9CB), one standard nematic LC pentylcyanobiphenyl (5CB) (Merck), and the chiral left-handed additive S811 (Merck). Furthermore, laser dyes, either DCM or LD688 (both purchased from Exciton), were added to the resulting CLC. Experimentally measured fluorescence emission and absorption spectra of described mixtures are shown in Fig. 2. For the mixture with DCM, the absorption peak is ∼460 nm and the fluorescence peak is ∼600 nm; for the mixture with LD688, the absorption peak is ∼525 nm, and the fluorescence peak is ∼650 nm.

The samples were prepared as sandwich-type cells with a slab of CLC_{OH} of thickness 50 μm confined between two glass plates with transparent electrode coatings. Thinner cells result in lower reflectivity of light. A strong electric field of amplitude ∼2.0 V/μm above some critical threshold E_{NCh} unwinds the CLC_{OH} into a uniform homeotropic nematic texture with the director parallel to the field (28). Such a state appears dark between crossed polarizers as shown in Fig. 3*A*; it has no photonic bandgap for lasing. At smaller fields, $E < E_{NCh}$, the director twists into the CLC_{OH} structure, which shows selective reflection of light, electrically tunable from near-UV through visible to near-IR range (Fig. 3 *B–D*). Mirrorless lasing occurs when the CLC_{OH} photonic bandgap matches with the fluorescent emission band of the laser dye (see *Supporting Information*).

The samples were pumped with 7-ns pulses at 532 nm from a frequency-doubled Q-switched Nd:YAG (neodymium-doped yttrium aluminium garnet) laser. An obliquely incident (at 45°) pump beam produces lasing emission from a CLC_{OH} sample in the direction of the helical axis. The two beams can be seen as spatially separated on a projection screen (Fig. 1*C*). The absorption bands of both dyes allow optical pumping at 532 nm, and the fluorescence bands provide lasing in the red range of visible spectrum (Fig. 2).

Fig. 4 illustrates the electric-field–dependent shift of the selective reflection band together with the effects of lasing and electric tunability of the emission wavelength. For example, in the mixture with DCM (Fig. 4*A*) with an electric field of 1.08 V/μm, the reflection band of the sample is centered at $\lambda_{max} = 565$ nm, and the lasing wavelength $\bar{\lambda}$ is observed at 575 nm. As the field is decreased to 0.92 V/μm, the reflection band center shifts to $\lambda_{max} = 664$ nm and $\bar{\lambda}$ increases to 675 nm. Note that λ_{max} is directly related to the electrically tunable pitch, $\lambda_{max} = \bar{n}p$, where $\bar{n} \approx 1.6$ is the average refractive index of the mixture. The fastest time of switching, ∼1 s, between different wavelengths of reflection and emission is achieved by using an intermediate state in which the director is completely unwound by the applied electric field, as discussed previously (29).

With the optical pump, lasing emission with a typical full width at half maximum (FWHM) in the range 0.09–0.33 nm occurs at the low-energy edge of CLC_{OH} bandgap (Fig. 4*A*). The lasing emission beam profiles, with pump energy 1.0 μJ per pulse from LD688-doped sample, and 10.0 μJ per pulse from DCM-doped sample, are observed using a beam profiling camera (Fig. 4*B*) and on a projection screen (Fig. 4*C*), respectively. Fig. 4*B* shows a narrow emission beam parallel to the CLC_{OH} helical axis. Such an emission is clearly distinguishable from a broad omnidirectional fluorescence. Fig. 4*C* demonstrates different colors of the emission beam projected as spots on a screen, obtained at different values of the applied electric field.

The CLC_{OH} laser emission shows a clear threshold as a function of pump energy, thus confirming lasing (Fig. 5*A*). The lasing threshold is $U_{th} = 0.23$ μJ per pulse at $\bar{\lambda} = 625$ nm for the LD688 sample, and $U_{th} = 1.55$ μJ per pulse at $\bar{\lambda} = 610$ nm for the DCM sample. In terms of fluence defined as $H_e = U_{th} \times \tau/(\pi \times w_0^2)$, where τ is pulse width of pump laser beam and w_0 is beam waist at

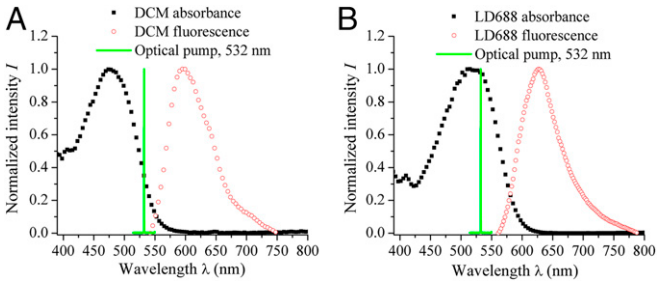

Fig. 2. Absorbance and fluorescence spectra of laser dyes in CLC mixtures. (*A*) DCM, (*B*) LD688. All plots are normalized by the maximum measured absorbance/fluorescence.

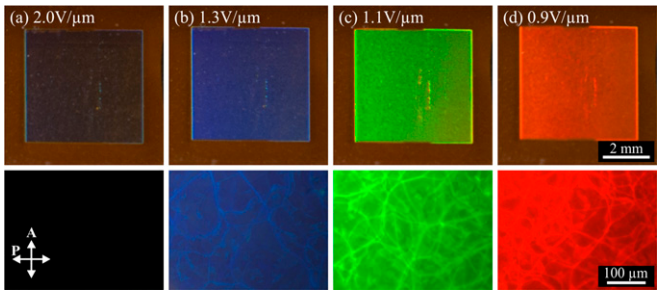

Fig. 3. Electric-field-controlled selective reflection of light in DCM-doped CLC mixture. Photographs in ambient light condition and corresponding polarizing optical micrographs of DCM sample cell with the following structures: (*A*) Electric field unwound homeotropic state; Electric-field-induced CLC_{OH} states reflecting (*B*) blue, (*C*) green, and (*D*) red visible light. The field values indicated are rms.

the sample, these lasing thresholds correspond to 2.20×10^{-7} J/m^2 for LD688 and 1.48×10^{-6} J/m^2 for DCM sample. The lower threshold for LD688 is related to its higher absorbance and concentration compared with that of DCM. With pump energies well above the threshold, laser emission can also appear at the high-energy band edge or even in the middle of the selective reflection band. Such a behavior can be caused by dislocations that adjust the CLC_{OH} structure whenever the pitch is tuned by the electric field and also by possible thermal degradation of the distributed feedback cavity. The laser emission is left-circularly polarized, consistent with the chirality of CLC_{OH} structure, thus indicating an optical feedback through internal Bragg reflection.

The use of an applied electric field to control the spectral location of the photonic bandgap in the CLC_{OH} structure while preserving the periodic heliconical conformation of the director provides an efficient mechanism to tune the wavelength of laser emission as long as the photonic bandgap overlaps the fluorescent emission spectrum of the laser dye (Fig. 4). In CLC_{OH} samples, $p \propto 1/E$; see refs. 26, 27. Below E_{NCh}, as the field decreases, the pitch increases, and the emission wavelength $\bar{\lambda}$ follows the spectral position of the selective reflection band, moving toward longer wavelengths (Figs. 4 *A* and 5 *B*). The tunability is extraordinarily broad, as $\bar{\lambda}$ changes in the range 574–675 nm in a mixture with the DCM dye, and 594–722 nm in the LD688 mixture (Fig. 5*B*). The tunable lasing range covers a large portion of the fluorescence band for each of the laser dyes (Fig. 2). In principle, with suitable laser dyes and pump source there is no limitation other than dispersion to extending lasing into different regions of the spectrum.

To demonstrate the efficiency of electrical tuning of laser emission from the CLC_{OH} structure, the lasing threshold was determined at different emission wavelengths for LD688 samples. The threshold is lowest near the fluorescence peak of the laser dye and increases near the two edges of the fluorescence band (Fig. 5*C*). When the overlap of selective reflection and fluorescence band diminishes, lasing becomes inefficient and unstable, with large variations in energy output from consecutive pump pulses. Moving the selective reflection band away from the fluorescence band completely eliminates lasing, leaving only a broad fluorescence in the emission spectrum. The intensity of laser emission from CLC_{OH} structure was measured as a function of emission wavelength for LD688 samples under a fixed pump energy of 8.6 ± 0.6 μJ per pulse. The energy of emitted laser pulses peaks near the center of the dye fluorescence band and decays as the selective reflection band is tuned away from it (Fig. 5*C*).

To conclude, we have demonstrated efficient electrically tunable lasing from the CLC_{OH} structure at room temperature. The principal advantage of the electrically controlled CLC_{OH} laser is that the electric field is applied parallel to the helical axis and thus changes the pitch but preserves the single-harmonic structure. The preserved single-harmonic periodicity explains why the efficiency of lasing is high in the entire tunable range of emission. The optically pumped CLC_{OH} laser is very simple to fabricate and operate, as it consists only of a thin slab of CLC material doped with a dye, confined between two glass plates with transparent electrodes. A known problem of all dye-based lasers is optical fatigue of dyes. Simplicity of the CLC_{OH} laser design allows one to overcome the problem by moving the CLC_{OH} cell and the pumping beam with respect to each other (30, 31). We achieved a very broad range of tunable lasing, exceeding 100 nm for each of the two dyes used. The broad tuning range of CLC_{OH} lasers, coupled with their microscopic size and narrow line widths, may enable new applications

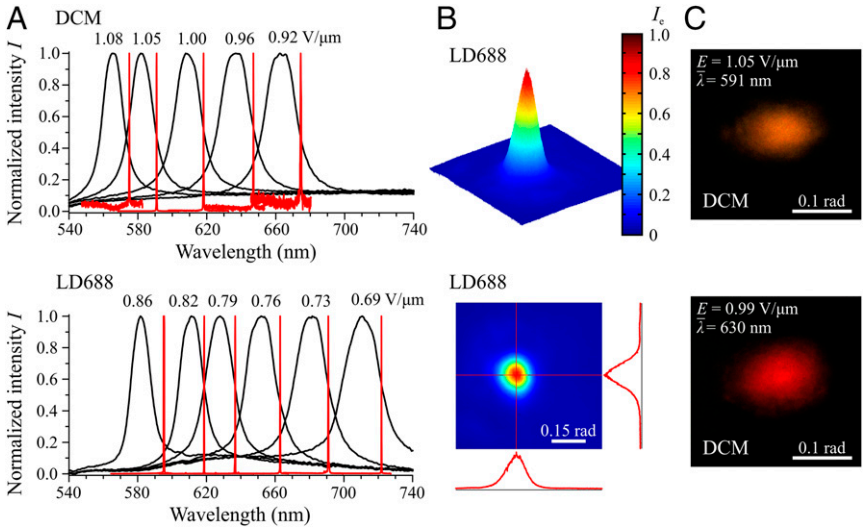

Fig. 4. Electrically tunable lasing from CLC_{OH} structure. (*A*) Reflection bands with associated lasing lines for DCM dye- (*Top*) and LD688 dye- (*Bottom*) doped samples at different electric fields. (*B*) Lasing emission beam profile with low pump energy and from a lasing spot of LD688-doped sample, E = 0.78 V/ μm, detected 25 mm away from the sample. (*C*) The lasing emission beam from a DCM-doped sample observed on a projection screen, positioned 75 mm from the sample, E = 1.05 V/μm for $\bar{\lambda} = 591$ nm, and E = 0.99 V/μm for $\bar{\lambda} = 630$ nm.

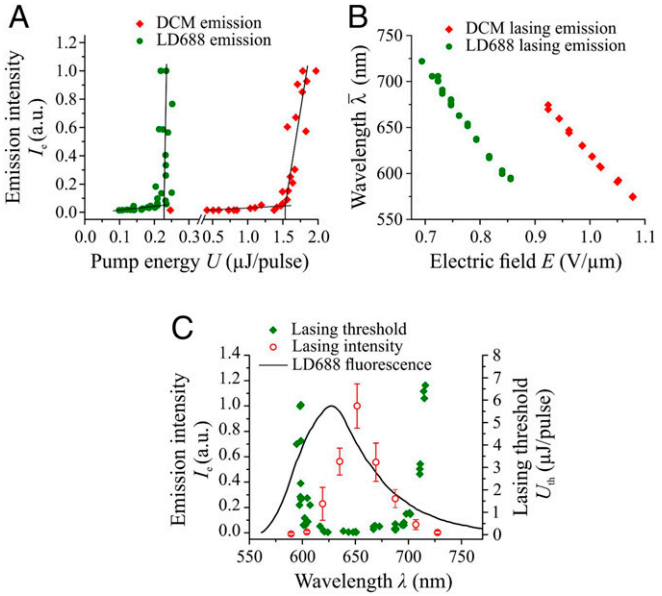

Fig. 5. Lasing efficiency and electrically tunable lasing range. (*A*) Lasing emission intensity as function of pump energy at $\bar{\lambda} = 610$ nm for DCM sample, and at $\bar{\lambda} = 625$ nm for LD688 sample. (*B*) Electric field dependence of the lasing wavelength $\bar{\lambda}$ for DCM and LD688 dye-doped CLC_{OH} samples. (*C*) Lasing threshold and intensity as function of lasing wavelength for LD688 sample. Error bars represent SD of lasing emission energy for 40 consecutive pump pulses.

in areas such as laboratories-on-a-chip, multicolor imaging, medical diagnostics, dermatology, and holography.

Methods

The main components of the explored mixtures that yield the necessary smallness of K_3 are CB7CB and CB9CB. The CB7CB shows a uniaxial N phase in the range (103–116) °C between the isotropic and the twist–bend nematic phase N_{tb}, while CB9CB is in the uniaxial N state in the range (105–121) °C. The dielectric anisotropy of both CB7CB and CB9CB is positive. Laser dyes DCM and LD688 are known to exhibit high photoluminescence efficiency; they are both soluble in the LC mixtures. Two mixtures were used, with composition CB7CB:CB9CB:5CB:S811:DCM (in weight units) being 29.9:19.9:45.9:4:0.3 [mixture DCM, cholesteric phase in the range (21–64) °C]; and CB7CB:CB9CB:5CB:S811:LD688 composition being 29.9:19.9:45.6:4:0.6 (mixture LD688, 29.5–62.8 °C). The average refractive index of the mixture is 1.6 as measured in the laboratory; elastic and dielectric properties are close to those reported earlier for similar CLC_{OH} materials (28, 29). The mixtures were thoroughly mixed before they were capillary-filled into the cells in the isotropic phase. The thickness of all of the LC cells was 50 ± 2 μm. All data reported below were obtained at 25 °C for the mixture with DCM, and 32.5 °C for the mixture with LD688. Experimentally measured fluorescence emission and absorption spectra of the mixtures are shown in Fig. 2. For the DCM mixture, the absorption peak is ∼460 nm, and fluorescence peak is ∼600 nm; for the LD688 mixture, the absorption peak is ∼525 nm, and fluorescence peak is ∼650 nm.

The temperature of the samples during lasing experiments was controlled by a laboratory-made hot stage with 0.1 °C accuracy. All cells were driven by the ac electric field of frequency 3 kHz (square wave). Flat cells were formed by glass plates with transparent indium tin oxide electrodes and an alignment layer of polyimide SE-1211 (Nissan). The field-induced color changes were visualized under the polarizing microscope (Optiphot2-pol, Nikon) with two crossed linear polarizers, in the reflection mode (Fig. 3 *B–D*).

To obtain electrically tunable lasing emission, the cells were optically pumped using a pulsed frequency-doubled Nd:YAG laser (Quantel YG682S-100) with a wavelength of 532 nm. The pulse width and the repetition rate of a pump beam were 7.5 ns and 2 Hz, respectively. The pump beam was focused on the cell to a ∼50-μm waist at an oblique incidence of ∼45° from the normal to the cell substrates. The output lasing emission along the normal forward direction of the cell was collected into an optical fiber and analyzed using a high-resolution spectrometer TRIAX 550 (Jobin Yvon Inc.) with optical resolution of 0.07 nm. The pump energy incident on the sample cell was controlled using a polarizer and analyzer. The absorbance spectra were measured using a fiber spectrometer USB4000 (Ocean Optics), and fluorescence spectra were measured using a TRIAX 550 spectrometer. The energies of the pump beam and laser emission were measured with Molectron energy meter OM4001.

ACKNOWLEDGMENTS. We are grateful to V. A. Belyakov and S. V. Shiyanovskii for useful discussions and to G. Cukrov for the measurements of refractive indices. CB9CB was synthesized by the Organic Synthesis Facility at the Liquid Crystal Institute, Kent State University. This work was supported by National Science Foundation DMR 1410378.

1. de Gennes PG, Prost J (1993) *The Physics of Liquid Crystals* (Clarendon, Oxford), pp 13–16.
2. Coles H, Morris S (2010) Liquid-crystal lasers. *Nat Photonics* 4(10):676–685.
3. Kopp VI, Fan B, Vithana HKM, Genack AZ (1998) Low-threshold lasing at the edge of a photonic stop band in cholesteric liquid crystals. *Opt Lett* 23(21):1707–1709.
4. Taheri B, Munoz AF, Palffy-Muhoray P, Twieg R (2001) Low threshold lasing in cholesteric liquid crystals. *Mol Cryst Liq Cryst (Phila Pa)* 358:73–82.
5. Palffy-Muhoay P, Cao WY, Moreira M, Taheri B, Munoz A (2006) Photonics and lasing in liquid crystal materials. *Philos Trans R Soc, A* 364(1847):2747–2761.
6. Morris SM, et al. (2006) The emission characteristics of liquid-crystal lasers. *J Soc Inf Disp* 14(6):565–573.
7. Funamoto K, Ozaki M, Yoshino K (2003) Discontinuous shift of lasing wavelength with temperature in cholesteric liquid crystal. *Jpn J Appl Phys* 42(12B):1523–1525.
8. Moreira MF, et al. (2004) Cholesteric liquid-crystal laser as an optic fiber-based temperature sensor. *Appl Phys Lett* 85(14):2691–2693.
9. Chanishvili A, et al. (2005) Widely tunable ultraviolet-visible liquid crystal laser. *Appl Phys Lett* 86(5):051107.
10. Sonoyama K, Takanishi Y, Ishikawa K, Takezoe H (2007) Position-sensitive cholesteric liquid crystal dye laser covering a full visible range. *Jpn J Appl Phys* 46(36-40):874–876.
11. Wang CT, Lin TH (2008) Multi-wavelength laser emission in dye-doped photonic liquid crystals. *Opt Express* 16(22):18334–18339.
12. Finkelmann H, Kim ST, Munoz A, Palffy-Muhoray P, Taheri B (2001) Tunable mirrorless lasing in cholesteric liquid crystalline elastomers. *Adv Mater* 13(14):1069–1072.
13. Schmidtke J, Kniesel S, Finkelmann H (2005) Probing the photonic properties of a cholesteric elastomer under biaxial stress. *Macromolecules* 38(4):1357–1363.
14. Varanytsia A, Nagai H, Urayama K, Palffy-Muhoray P (2015) Tunable lasing in cholesteric liquid crystal elastomers with accurate measurements of strain. *Sci Rep* 5: 17739.
15. Chanishvili A, et al. (2003) Phototunable lasing in dye-doped cholesteric liquid crystals. *Appl Phys Lett* 83(26):5353–5355.
16. Furumi S, Yokoyama S, Otomo A, Mashiko S (2004) Phototunable photonic bandgap in a chiral liquid crystal laser device. *Appl Phys Lett* 84(14):2491–2493.
17. Furumi S, Yokoyama S, Otomo A, Mashiko S (2003) Electrical control of the structure and lasing in chiral photonic band-gap liquid crystals. *Appl Phys Lett* 82(1):16–18.
18. Ozaki M, et al. (2003) Electro-tunable liquid-crystal laser. *Adv Mater* 15(12):974–977.
19. Yu H, Tang B, Li J, Li L (2005) Electrically tunable lasers made from electro-optically active photonics band gap materials. *Opt Express* 13(18):7243–7249.
20. Inoue Y, et al. (2010) Electric field dependence of lasing wavelength in cholesteric liquid crystal with an in-plane helix alignment. *Mol Cryst Liq Cryst (Phila Pa)* 516: 182–189.
21. Park B, et al. (2009) Electrically controllable omnidirectional laser emission from a helical-polymer network composite film. *Adv Mater* 21(7):771–775.
22. Lin TH, et al. (2006) Electrically controllable laser based on cholesteric liquid crystal with negative dielectric anisotropy. *Appl Phys Lett* 88(6):061122.
23. Schmidtke J, Junnemann G, Keuker-Baumann S, Kitzerow HS (2012) Electrical fine tuning of liquid crystal lasers. *Appl Phys Lett* 101(5):051117.
24. Palto SP, et al. (2011) Photonics of liquid-crystal structures: A review. *Crystallogr Rep* 56(4):622–649.
25. Strangi G, et al. (2005) Color-tunable organic microcavity laser array using distributed feedback. *Phys Rev Lett* 94(6):063903.
26. de Gennes PG (1968) Calcul de la distorsion d'une structure cholesterique par un champ magnetique. *Solid State Commun* 6(3):163–165.
27. Meyer RB (1968) Effects of electric and magnetic fields on the structure of cholesteric liquid crystals. *Appl Phys Lett* 12(9):281–282.
28. Xiang J, Shiyanovskii SV, Imrie CT, Lavrentovich OD (2014) Electrooptic response of chiral nematic liquid crystals with oblique helicoidal director. *Phys Rev Lett* 112(21): 217801.
29. Xiang J, et al. (2015) Electrically tunable selective reflection of light from ultraviolet to visible and infrared by heliconical cholesterics. *Adv Mater* 27(19):3014–3018.
30. Chilaya G, et al. (2006) Enhancing cholesteric liquid crystal laser stability by cell rotation. *Opt Express* 14(21):9939–9943.
31. Wood SM, et al. (2013) Adaptive holographic pumping of thin-film organic lasers. *Opt Lett* 38(21):4483–4486.
32. Dolganov PV (2015) Density of photonic states in cholesteric liquid crystals. *Phys Rev E Stat Nonlin Soft Matter Phys* 91(4):042509.
33. Varanytsia A, Palffy-Muhoray P (2013) Thermal degradation of the distributed-feedback cavity in cholesteric liquid crystal lasers. *Proc SPIE* 8828:88281F.